Effect of superlattice structure on the thermoelectric figure of merit

D. A. Broido
Department of Physics, Boston College, Chestnut Hill, Massachusetts 02167

T. L. Reinecke
Naval Research Laboratory, Washington, D.C. 20375

(Received 1 December 1994)

The electrical conductivity, the thermoelectric power, and the electrical contribution to the thermal conductivity of superlattices have been studied within the envelope-function approach for the electrons. The effects of tunneling through the barriers due to finite potential offsets and of the thermal currents through the barrier layers are shown to be essential to describe properly the thermoelectric figure of merit of realistic superlattices. The figure of merit is calculated as a function of superlattice period, potential barrier offset, and barrier width. It is found that the figure of merit has a maximum as a function of superlattice period and that its value there can be somewhat larger than that of the corresponding bulk. For larger periods the figure of merit is generally less than that of the correponding bulk.

INTRODUCTION

Recently there has been increased interest in finding additional materials for use in cleaner, more efficient cooling systems.[1] For some time the materials that have shown the most promise have been alloys of Bi_2Te_3. The dimensionless figure of merit[2] ZT provides a measure of the desirability of a material for use in cooling systems. It is given by $ZT=\alpha^2\sigma T/\kappa$, where α is the thermoelectric power, σ the electrical conductivity, κ the total thermal conductivity, and T is the temperature. Even modest improvements in ZT would be quite desirable for a number of applications. Currently several avenues are being investigated in the pursuit of improved thermoelectric materials.[3-6] Nevertheless, in recent years little improvement in the figure of merit of thermoelectric materials over those of Bi_2Te_3 alloys, which have $ZT \lesssim 1$, has been achieved.

Calculations of the thermopower[7] and other transport properties of superlattice systems have been reported over the years. Recently, however, Hicks and coworkers[8,9] have proposed that very large increases in ZT can be achieved in superlattices for conduction parallel to the planes. This work has attracted considerable attention in the thermoelectrics community because of the appearance that superlattice systems may be highly desirable for applications, and in the superlattice community because of the unusual transport properties predicted for these systems. The physical origin of the large increase in ZT proposed for these superlattice systems comes mainly from the large density of electron states per unit volume that occurs for small well widths in a quasi-two-dimensional geometry. This density of states is given by $m/\pi\hbar^2 a$, where m is the carrier mass and a is the quantum-well width. These authors[8] made calculations for what are essentially superlattices composed of layers of materials having two-dimensional electronic properties given by infinite potential barriers and zero barrier widths, and they found that ZT increased dramatically for decreasing well widths.

Such a treatment, however, neglects two physical effects, which we show here are essential to describe the figure of merit of realistic superlattice systems. They are (i) that thermal current flows through the barrier layers in addition to the well layers, whereas electrical current is associated mainly with the wells, thus giving a decreased overall electrical conductivity and decreased ZT, and (ii) that electron tunneling occurs between the layers, especially for superlattices with small periods, which modifies the density of states and gives a decreased ZT. Recently Lin-Chung and Reinecke[10] addressed the first issue with model calculations in which layers with quasi-two-dimensional electronic properties without tunneling were separated by barriers of finite width, and they found that the thermal transport through the barriers reduces ZT considerably.[11]

In the present work we have addressed these two issues in a unified way, and have produced a description of ZT of realistic superlattice systems. The electronic properties have been calculated including finite potential barriers, and the transport properties have been obtained including the finite widths of the barriers. We find that these effects substantially decrease ZT for superlattices as compared to those for quasi-two-dimensional systems. ZT for superlattices has a maximum, which can be greater than the bulk value, for small superlattice periods, and it generally is smaller than the bulk value for larger periods.

CALCULATIONS

The coupled equations for the electrical and heat currents $\mathbf{J}_e$ and $\mathbf{J}_s$ are given in terms of the gradients of the electrostatic potential ϕ and temperature T by[4]

$$\begin{bmatrix} -\mathbf{J}_e/e \\ -\mathbf{J}_s/k_B \end{bmatrix} = \begin{bmatrix} \frac{\sigma}{e^2} & \frac{\sigma\alpha}{ek_B} \\ \frac{\sigma\alpha T}{ek_B} & \frac{\gamma}{k_B^2} \end{bmatrix} \begin{bmatrix} \nabla(e\phi) \\ \nabla(k_B T) \end{bmatrix}, \tag{1}$$

where σ, γ, and α, respectively, are the electrical conduc-

tivity, the electrical contribution to the thermal conductivity at zero field, and the thermoelectric power, and in general they are 3×3 matrices in the Cartesian coordinates. In the relaxation-time approximation to the Boltzmann equation, these quantities can be expressed as[12]

$$\sigma=L_0,\quad \sigma\alpha=-\frac{1}{eT}L_1,\quad \gamma=\frac{1}{e^2T}L_2\ , \tag{2}$$

and the thermal conductivity at zero current is $\kappa_e=\gamma-T\sigma\alpha^2$. It should be noted that the total thermal conductivity is composed of a phonon part in addition to the electronic contribution, $\kappa=\kappa_{\rm ph}+\kappa_e$. In Eq. (2),

$$L_j=\int d\varepsilon\left[-\frac{\partial f_0}{\partial\varepsilon}\right]\chi(\varepsilon)(\varepsilon-\zeta)^j \tag{3}$$

and

$$\chi(\varepsilon)=e^2\tau(\varepsilon)\int\frac{d\mathbf{k}}{4\pi^3}\delta[\varepsilon-\varepsilon(\mathbf{k})]v_x^2\ , \tag{4}$$

where $\tau(\varepsilon)$ is the relaxation time, $\varepsilon(\mathbf{k})$ is the dispersion relation of an electron in the conduction band, $\mathbf{k}=(k_x,k_y,k_z)$ is a three-dimensional wave vector, f_0 is the equilibrium Fermi distribution, $v_x=\hbar^{-1}\partial\varepsilon(\mathbf{k})/\partial k_x$, and ζ is the chemical potential of the carriers. We have taken the transport to be in the x direction.

Here we are primarily interested in the effects of carrier confinement in realistic superlattices having finite barrier heights and nonzero barrier widths. In order to address these issues we have made calculations for superlattices with periods $d=a+b$, where a and b are the widths of the quantum well and the barrier, respectively, and V_0 is the conduction-band offset in the barrier. For simplicity we assume that the well material and the barrier material are each characterized by a single parabolic but anisotropic conduction band, and we take the carrier masses, mobilities, and phonon thermal conductivities of the barrier material to be the same as those of the quantum well. That is, the essential effect that we study is the modification of the bulk electronic band structure into a superlattice band structure, which is modeled here by the potential offset in the barrier.

The calculations are done within the effective-mass approximation using a rectangular potential offset V_0 in the barrier regions. The resulting electronic energies are given by a set of Kronig-Penney-like subbands that derive from the bulk conduction band.[13] The dispersion of the ith subband is

$$\varepsilon_i(\mathbf{k})=\varepsilon_i(k_z)+\frac{\hbar^2}{2}\left[\frac{k_x^2}{m_x}+\frac{k_y^2}{m_y}\right]\ . \tag{5}$$

Here the superlattice axis is chosen to be the z direction, m_x and m_y are the anisotropic effective masses in the plane of the layers, and $\varepsilon_i(k_z)$ is obtained by solution of the Kronig-Penney model.

For relatively weak coupling between wells, $\varepsilon_i(k_z)$ can be approximated by

$$\varepsilon_i(k_z)=\varepsilon_{i0}+\Delta_i(1\mp\cos k_z d)\ , \tag{6}$$

where ε_{i0} is the energy at the bottom of the ith subband, the overlap integrals Δ_i give the half-width of the subband, and the $+$ $(-)$ sign corresponds to positive (negative) band dispersion. Δ_i depends on the potential height V_0, and the barrier and well widths a and b on the subband index i. For strong tunneling between wells, as occurs for small barrier widths and low barrier heights, Eq. (6) is in general not a good approximation. However, for the range of parameters a, b, and V_0 considered in this work, we find that Eq. (6) gives a good fit to the relevant portion[14] of the exact Kronig-Penney band structure. The density of states of the superlattice is then obtained analytically by summing over wave vectors at a given energy.[7] The density of states for each subband is

$$g_i(\varepsilon)=\frac{\sqrt{m_x m_y}}{\pi\hbar^2}\frac{1}{d}\begin{cases}\dfrac{d}{\pi}k_{zi}, & \varepsilon_{i0}<\varepsilon<\varepsilon_{i0}+2\Delta_i\\ 1, & \varepsilon>\varepsilon_{i0}+2\Delta_i\ ,\end{cases}$$
$$k_{zi}=\frac{1}{d}\cos^{-1}\left[1-\frac{\varepsilon-\varepsilon_{i0}}{\Delta_i}\right]\ . \tag{7}$$

Employing the superlattice band structure of Eq. (6), σ, α, and γ can be expressed as

$$\sigma=e\mu_x\sum_i\bar{n}_i\ , \tag{8}$$

$$\sigma\alpha=e\mu_x\sum_i[2\bar{\varepsilon}_i-(\Delta_i+\zeta_i)\bar{n}_i+\bar{\lambda}_i]\ , \tag{9}$$

$$\gamma=e\mu_x\sum_i[3\bar{\varepsilon}_i^2-2(\Delta_i+2\zeta_i)\bar{\varepsilon}_i+\zeta_i(2\Delta_i+\zeta_i)\bar{n}_i+2\bar{\phi}_i-2\zeta_i\bar{\lambda}_i]\ , \tag{10}$$

where

$$\bar{n}_i=\int_0^\infty d\varepsilon\, f_0(\varepsilon)g_i(\varepsilon)\ ,$$
$$\bar{\varepsilon}_i=\int_0^\infty d\varepsilon\, f_0(\varepsilon)g_i(\varepsilon)\varepsilon\ ,$$
$$\bar{\varepsilon}_i^2=\int_0^\infty d\varepsilon\, f_0(\varepsilon)g_i(\varepsilon)\varepsilon^2\ ,$$
$$\bar{\lambda}_i=\Delta_i\int_0^{2\Delta_i}d\varepsilon\, f_0(\varepsilon)g_i(\varepsilon)\left[\frac{\sin k_{zi}d}{k_{zi}d}\right]\ ,$$
$$\bar{\phi}_i=\Delta_i\int_0^{2\Delta_i}d\varepsilon\, f_0(\varepsilon)g_i(\varepsilon)\varepsilon\left[\frac{\sin k_{zi}d}{k_{zi}d}\right]\ .$$

In these expressions, the energy and chemical potential of the carriers $\zeta_i=(\zeta-\varepsilon_{i0})$ are measured from the bottom of the ith superlattice subband, and $\mu_x=e\tau/m_x$ is the carrier mobility. For simplicity, the relaxation time τ is assumed to be independent of energy and of subband index. For each set of superlattice parameters, the quantities, α, σ, and κ_e give ZT as a function of the chemical potential ζ.

To illustrate the effects of the superlattice band structure on ZT, calculations have been made for Bi_2Te_3 superlattices. The transport properties of Bi_2Te_3 are highly anisotropic. For this material, we take the x direction to be in the quantum-well plane and to be along the a_0 axis of the hexagonal unit cell. The superlattice direction, taken to be the z direction, is chosen to be along the b_0

axis of the unit cell, which gives[15] $m_x=0.021$, $m_y=0.32$, and $m_z=0.081$, and a mobility $\mu_x=1200$ cm^2/V s. Calculations were done at room temperature, $T=300$ K is assumed. The value of the phonon contribution to the thermal conductivity is[15] $\kappa_{ph}=0.015$ W/cm K for both the well and barrier materials.

RESULTS AND DISCUSSION

We have made calculations of ZT using the results for σ, α, and κ_e obtained from Eqs. (8)–(10) for superlattices and compared to the corresponding results for bulk materials. In each case, the chemical potential ζ is chosen so as to maximize ZT. In practice such variations in ζ can be obtained by changing the carrier densities through doping.

Figure 1 illustrates such results for ZT for the Bi_2Te_3 superlattice, ZT_S, as a function of the thickness of the quantum-well layer, a, for three different ratios, $b/a=\frac{1}{2}$, 1, and 2. The barrier height V_0 is taken to be 200 meV, a value that is typical of offsets in superlattices. The results are scaled to the bulk value for Bi_2Te_3, which is calculated to be $ZT_{3D}=0.53$.[16] For thicker wells, the ZT_S for the superlattice lies below that of the bulk, and this effect is more pronounced for the larger barrier thicknesses. This behavior arises from the parasitic effects of the thermal current that flows through the barrier layers. This effect is given by the $1/d=1/(a+b)$ dependence of σ, $\sigma\alpha$, and κ_e in Eqs. (8)–(10) through the density of states [Eq. (7)], where it is seen that the electrical and thermal currents per unit area decrease when the barrier width b becomes large. For decreasing well widths, ZT_S increases and reaches a maximum, and then for still smaller well widths ZT_S decreases as a result of carrier tunneling through the barriers. The value of the well width at which the maximum occurs decreases for increasing barrier widths b. The maximum of ZT_S for superlattices is found to be somewhat larger than the bulk value, and is nearly independent of the barrier width for this range a and b. This enhancement arises from changes in the density of states upon electron confinement in relatively narrow wells.

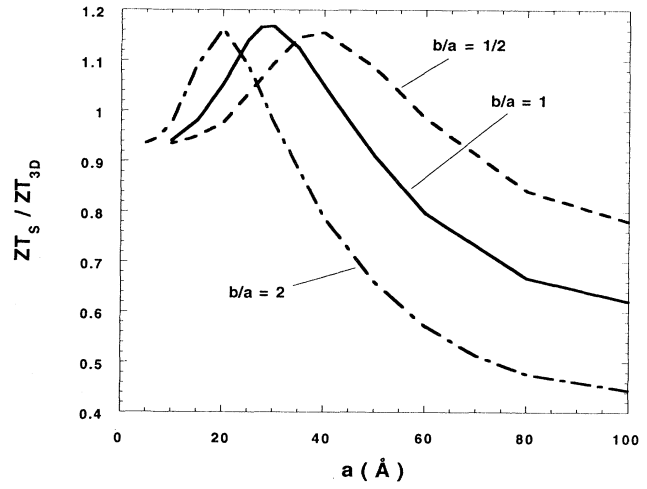

FIG. 1. The figure of merit ZT_S of Bi_2Te_3 superlattices scaled by ZT_{3D} for the corresponding bulk given as a function of the well width a for several ratios of the barrier width to well width, $b/a=\frac{1}{2}$ (dashed line), 1 (solid line), and 2 (dash-dotted line).

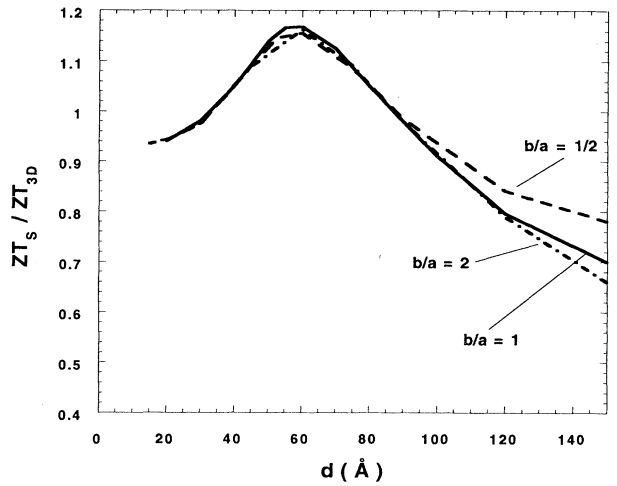

FIG. 2. The figure of merit ZT_S of Bi_2Te_3 superlattices (scaled by ZT_{3D}) as a function of the superlattice period $d=a+b$ for the ratios b/a given in Fig. 1.

Additional insight into the behavior shown in Fig. 1 can be obtained by examining ZT_S as a function of d, which is shown in Fig. 2. For values of d in the neighborhood of its maximum, ZT_S is found to depend only on d. This occurs because of the competing effects of confinement and tunneling.

Figure 3 illustrates the dependence of ZT_S on the barrier height V_0. For large periods d, ZT_S increases for decreasing V_0 and approaches the bulk value. In effect, the thermal conduction in the barriers becomes relatively less important as the carriers spread out into the barriers. For superlattice periods near the maximum of ZT_S, its

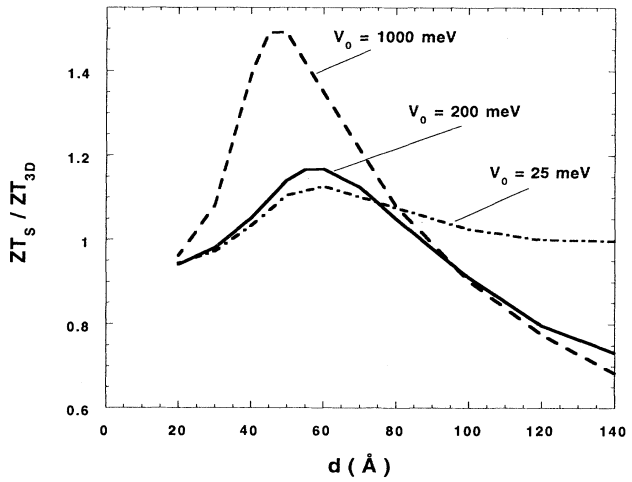

FIG. 3. The figure of merit ZT_S of Bi_2Te_3 superlattices (scaled by ZT_{3D}) as a function of the superlattice period d for several potential barrier heights, $V_0=25$ (dash-dotted line), 200 (solid line), and 1000 meV (dashed line).

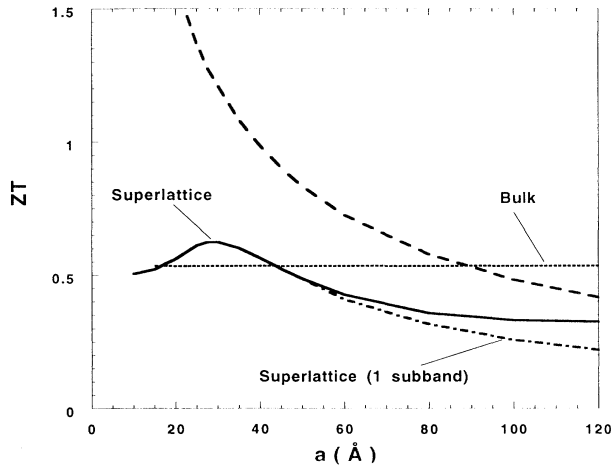

FIG. 4. The figure of merit ZT_S of Bi_2Te_3 superlattices as a function of the well width a. The dotted curve is for bulk Bi_2Te_3. The solid curve is for superlattices with $b/a=1$ and $V_0=200$ meV. The dashed-dotted curve gives similar results for superlattices but including only carriers in the lowest Kronig-Penney band. The dashed curve is for superlattices with infinite potential offsets and zero barrier widths, like those studied in Ref. 8.

enhancement over the bulk value is larger for larger V_0, which arises from greater quantum confinement manifested by flatter superlattice dispersions. For an infinitely large V_0, ZT_S continues to increase for decreasing d (not shown in the figure). This shows that within the present approach the existence of a maximum in ZT_S as a function of d (or of a) arises from tunneling between the layers, and the enhancement over the bulk value arises from quantum confinement effects.

Figure 4 compares the ZT_S for Bi_2Te_3 superlattices having $V_0=200$ meV directly with the bulk case. For well widths $\gtrsim 40$ Å, ZT_S is smaller than that for the corresponding bulk, which is expected from the increased effects of the thermal current through the barriers relative to the electrical current. We also note in Fig. 4 that if only a single Kronig-Penney band is taken into account in the calculations, rather than all thermally occupied bands, a smaller value of ZT_S is obtained for wider well widths.[17] Physically, as more subbands are included the effective density of states at a given energy increases.

Results like those of Hicks and Dresselhaus,[8] which were made for infinite potential barriers and zero barrier widths, and including only one electron subband, are shown by the dashed line in Fig. 4. The lower overall values obtained here for ZT_S as compared to those in the dashed curve are a consequence of our inclusion of thermal currents in the barriers, and the decrease of ZT_S for small well widths arises from our inclusion of carrier tunneling between wells.

In summary, a theoretical treatment of the thermoelectric transport properties and the thermoelectric figure of merit of realistic superlattice systems has been given here. Increases in the figure of merit as compared to the bulk are found for relatively small superlattice periods. It has been shown that it is essential to include the effects of thermal transport in the barrier layer and of carrier tunneling between layers in order to obtain a proper description of these systems. These effects considerably decrease the figure of merit of realistic systems as compared to that of layers having fully two-dimensional electronic properties. In principle, larger values of ZT can be obtained in superlattices with high potential barriers or with barrier layers having low thermal conductivities.

ACKNOWLEDGMENT

This work was supported in part by the U.S. Office of Naval Research (TLR).

[1]C. Wood, Rep. Prog. Phys. **51**, 459 (1988).
[2]H. J. Goldsmidt, *Thermoelectric Refrigeration* (Plenum, New York, 1964).
[3]G. A. Slack, in *Solid State Physics,* edited by H. Ehrenreich, F. Seitz, and D. Turnbull (Academic, New York, 1979), Vol. 34.
[4]D. J. Bergman and O. Levy, J. Appl. Phys. **70**, 6821 (1991).
[5]G. D. Mahan, J. Appl. Phys. **70**, 4551 (1991).
[6]G. A. Slack and V. G. Tsoukala, J. Appl. Phys. **76**, 1665 (1994).
[7]L. Friedman, J. Phys. C **17**, 3999 (1984); T. Tao and L. Friedman, *ibid.* **18**, L455 (1985).
[8]L. D. Hicks and M. S. Dresselhaus, Phys. Rev. B **47**, 12 727 (1993).
[9]L. D. Hicks, T. C. Harman, and M. S. Dresselhaus, Appl. Phys. Lett. **63**, 3230 (1993).
[10]P. J. Lin-Chung and T. L. Reinecke, Phys. Rev. B **51**, 13 244 (1995).
[11]Recently Mahan and Lyon [G. D. Mahan and H. B. Lyon, J. Appl. Phys. **76**, 1899 (1994)] also discussed the role of heat transport in the barriers of superlattices.
[12]N. W. Ashcroft and N. D. Mermin, *Solid State Physics* (Saunders, Philadelphia, 1976), Chap. 13.
[13]C. Kittel, *Introduction to Solid State Physics* (Wiley, New York, 1986), Chap. 7.
[14]That portion of the band structure that is occupied by carriers.
[15]The values of the parameters for Bi_2Te_3 are given in Ref. 8.
[16]To take into account the six valleys of the conduction band of Bi_2Te_3, σ and κ_e have been multiplied by 6 for both bulk and superlattices. For the superlattices, this is expected to be an overestimate of these quantities because the anisotropic masses partially lift the valley degeneracy.
[17]In the present calculations only intrasubband electron scattering is taken into account.